PROCEEDINGS OF SCIENCE

Measurement of Higgs boson production and properties

Chiara Arcangeletti[a,*] **for the ATLAS and CMS collaborations**
[a] *INFN Laboratori Nazionali di Frascati, Frascati, Italy*
E-mail: chiara.arcangeletti@cern.ch

With the ATLAS and CMS detectors at LHC, a proton-proton collision dataset collected at $\sqrt{s}$=13 TeV reached an integrated luminosity of about 140 fb^{-1}. This dataset allows to study the Higgs boson properties in different Higgs boson decay channels with unprecedented precision. The latest measurements of the Higgs boson mass, CP, width, and couplings as well as self-couplings are presented, together with the simplified template cross sections and the fiducial cross section, for which a first measurement at 13.6 TeV is shown.

The Eleventh Annual Conference on Large Hadron Collider Physics (LHCP2023)
22-26 May 2023
Belgrade, Serbia

[*] Speaker

PoS(LHCP2023)227

1. Introduction

From the discovery of the Higgs boson claimed by the ATLAS [1] and CMS [2] experiment in 2012, several studies have been carried out to compare its properties with those predicted by the Standard Model (SM). Higgs boson properties, such as its interactions with SM fermions and bosons, can be examined within its primary production processes: gluon fusion (ggF), vector boson fusion (VBF), associated production with W or Z bosons (WH, ZH), or in association with a pair of top quarks ($t\bar{t}H$); as well as in its decay modes, including $H \rightarrow ZZ$, WW, $\gamma\gamma$, $\tau\tau$, bb, $Z\gamma$, and $\mu\mu$. During Run 1, the combined ATLAS and CMS measurements of the Higgs boson's production and decay rates, coupled with constraints on its interactions with vector bosons and fermions, were undertaken [3]. These outcomes were interpreted in terms of the "signal strength," representing the ratio of the observed cross section (σ) times branching ratio (BR) concerning the SM's expected value. The Higgs boson's production and decay rates can be parametrized within the "κ-framework" [4], wherein the $\sigma \times BR$ values are computed in relation to coupling modifiers κ," which serve as scaling factors for cross sections and partial widths. With the increasing statistics of the Run 2 up to 139 fb^{-1}, substantial advancements have been made in the precision of property measurements. These improvements encompass measurements related to the Higgs boson's mass, spin/CP properties, width, fiducial differential cross sections, and production cross sections. Interpretations of the results have been extended to various theoretical frameworks, including the Effective Field Theory (EFT), in addition to the "κ-framework." These extensions aid in establishing constraints on anomalous Higgs boson couplings with other SM particles and probing New Physics phenomena. Notably, the expanded dataset has led to initial evidence of exceedingly rare processes, such as the Higgs boson decaying into Zγ, and has set constraints on the self-coupling of the Higgs boson.

2. Higgs boson precision measurements

2.1 Higgs boson Mass

The Higgs boson mass measurement has been performed in two of the most sensitive channels $H \rightarrow ZZ^* \rightarrow 4l$ and $H \rightarrow \gamma\gamma$, due their clear signature and a mass resolution of 1-2%. Due to their low BR, the total uncertainties on the mass measurement are dominated by the statistical term, and the systematic ones by the experimental effects related to the muon momentum and photon energy scales. The latest results from CMS experiment in the two channels with the partial Run 2 statistics of 35.9 fb^{-1} has been combined with the Run 1 results to obtain the combined measurement of the Higgs boson mass: $m_{\rm H} = 125.38 \pm 0.14$ (± 0.11) GeV [5]. While the ATLAS experiment published the mass measurement in $H \rightarrow ZZ^* \rightarrow 4l$ channel with the full Run 2 statistics, also combined with Run 1 dataset: $m_{\rm H} = 124.94 \pm 0.18$ (± 0.17) GeV [6].

2.2 Higgs boson CP structure

Both ATLAS and CMS investigated CP-violation in the Higgs sector by studying how the Higgs boson interacts with vector bosons and fermions. A common feature of those searches is the use of observables optimised to discriminate different CP hypothesis, since the only rate information cannot disentangle anomalous CP-even or CP-odd effect while observable shape does.

PoS(LHCP2023)227

Then the results are interpreted in terms of anomalous Higgs boson couplings. The HVV vertex has been studied mainly in the VBF production and in the $H \to ZZ*$ decay channel. ATLAS set limits on the the parameter $\tilde{d}$, which represents the strength of CP violation, studying the VBF production in the $H \to \gamma\gamma$ and $H \to \tau\tau$ decay channels. It has been constrained to the interval [-0.012,0.030] at the 68% CL, based on the fit of Optimal Observable distribution, a matrix element based variable able to discriminate CP-odd contribution [7]. Similar approach has been used also in constraining the HVV anomalous coupling in the SMEFT framework in the dedicated analysis studying both the VBF and the $H \to ZZ*$ vertex [8]. On the other hand, CMS set constraints on the CP-violating parameter f_{a3}, which is the effective fractional cross section, in the VBF production looking at the $H \to \tau\tau$ decay, and also combining with $H \to 4l$. The most stringent limits set are $f_{a3} = 0.20^{+0.26}_{-0.16} \times 10^{-3}$ at the 68% CL and they are obtained fitting the MELA observable [9].

For what concern instead the Hff couplings, the main vertices under investigations are the ttH/tH production as well as the $H \to \tau\tau$ decay. Both ATLAS and CMS set limits on the coupling modifier κ_t defining 2-dimensional confidence level. ATLAS measures a mixing angle between CP-even and CP-odd top-Higgs Yukawa couplings of $\alpha = 11^{\circ+52^\circ}_{-73^\circ}$ [10]. CMS measures instead a fraction CP-odd contribution $|f^{ttH}_{CP}| = 0.28$ with an interval of $|f^{ttH}_{CP}| < 0.55$ at the 68% CL [11]. Furthermore, ATLAS has measured the mixing angle ϕ_τ, which describe possible CP-violating interactions between the Higgs boson and τ lepton in the $H \to \tau\tau$ decay channel. It is measured to be $9^\circ \pm 16^\circ$ and the pure CP-odd hypothesis is disfavoured at the level of 3.4σ [12].

2.3 Higgs boson Width

A direct measurement of Higgs width is limited by the experimental resolution which is orders of magnitude greater than the one needed for the measurement. The $H \to ZZ^*$ decay channel sets a constraint on the Higgs boson width, obtained by measuring the off-shell Higgs boson production event yields normalised to the on-shell one $\mu_{\text{off-shell}}/\mu_{\text{on-shell}}$, assuming identical coupling modifiers for on-shell and off-shell Higgs boson. Both ATLAS and CMS performed the Higgs width measurement combining the results in the $ZZ^* \to 4l$ and $ZZ^* \to 2l2\nu$ decay channels, observing a $\Gamma_{\text{H}} = 4.5^{+3.3}_{-2.5}$ MeV at 68% CL [13] and $\Gamma_{\text{H}} = 3.2^{+2.4}_{-1.7}$ MeV at 68% CL [14] respectively. Furthermore both the experiments observed the first evidence of the off-shell Higgs production measuring an off-shell signal strength of $\mu_{\text{off-shell}} = 1.1 \pm 0.6$ (3.3σ) by ATLAS [13] and of $\mu_{\text{off-shell}} = 0.74^{+0.56}_{-0.38}$ (3.6σ) by CMS [14].

3. Higgs boson Fiducial Cross Section

3.1 Measurements at 13 TeV

Differential cross section measurement are performed on several variables sensitive to the Higgs boson properties related to the Higgs kinematics or to the jets produced in association. The distributions are unfolded, to correct for detector level effects, in a fiducial phase space based on detector acceptance to minimise the model dependency. Different phase space definition can be used to target different production modes. The CMS Collaboration recently published several differential cross section measurements in the $H \to ZZ^* \to 4l$ [15] and $H \to \gamma\gamma$ [16] with the full Run 2 statistics. In particular in the four lepton decay observables related to the four leptons

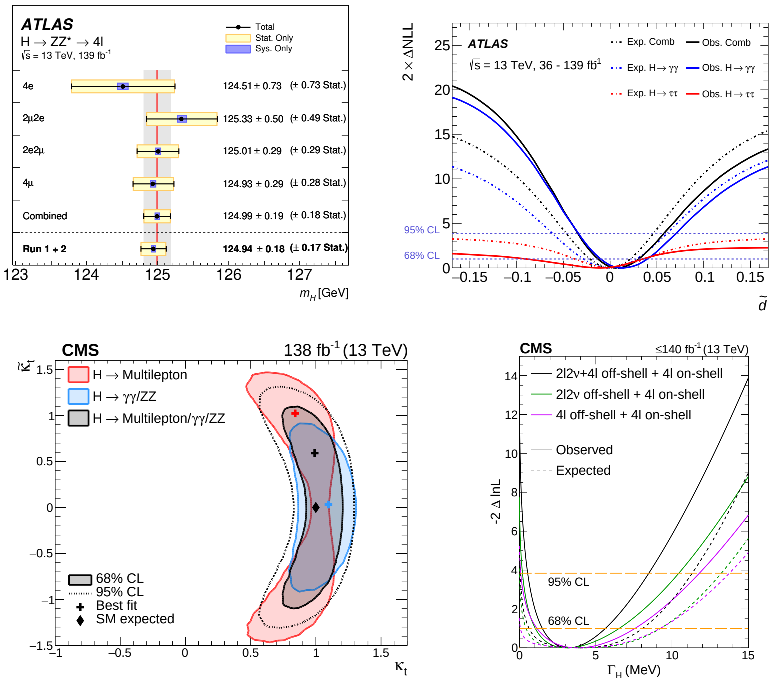

Figure 1: (top-left) Measured values of the Higgs boson mass by ATLAS for the Run 1 and Run 2 in $H \to ZZ^* \to 4l$ decay channel, as well as their combined results [6]. (top-right) The observed likelihood curve as function of $\tilde{d}$, compared with the expected curves, in the $H \to \gamma\gamma$ and $H \to \tau\tau$ and combined by ATLAS [7]. (bottom-left) The observed 2D likelihood contours for κ_t and $\tilde{\kappa}_t$ in the multilepton, $\gamma\gamma$ and ZZ^* final states from CMS [11]. (bottom-right) CMS likelihood scan of the Higgs width in $H \to ZZ^* \to 4l$ and $H \to ZZ^* \to 2l2\nu$ final states and their combination [14].

kinematics sensitive for testing the Higgs CP properties were studied. For example CMS unfolded the matrix element kinematic discriminant sensitive to anomalous HVV CP coupling [15] while ATLAS published the unfolded distribution of the Optimal Observables sensitive to CP-odd effects both at the decay as well as at the production vertex [8]. The results in this two channels have been combined by the ATLAS Collaboration [17], extrapolating the individual results to the full phase space. This implies larger theory uncertainties but lead to a sensible reduction of the statistical error which largely compensate the acceptance uncertainties. In this analysis, as well as in the CMS $H \to ZZ^* \to 4l$ one, the Higgs p_T spectrum were used to constrain the Yukawa couplings of the Higgs boson with the charm quark, which affects the low-p_T. The limits obtained by the CMS collaboration is $\kappa_c = [-5.3, 5.2]$ at 95% CL [15]. The ATLAS Collaboration combined the constrains obtained by the combination of the $H \to ZZ^* \to 4l$ and $H \to \gamma\gamma$ channels with the direct measurements in the VH, $H \to b\bar{b}$ and VH, $H \to c\bar{c}$ decay channels, obtaining tighter constraint of $\kappa_c = [-2.47, 2.53]$ at 95% CL [17]. Finally The ATLAS Collaboration also performed differential cross-section measurements with full Run 2 dataset in different phase spaces for the $H \to WW^* \to e\nu\mu\nu$ decay channel applying different requirements on the number of jets: $N_{jets} = 0, 1$ to target ggF production mode [18] and $N_{jets} \geq 2$ to target VBF one [19]. In the latter case the $\Delta\phi_{jj}$ and p_T^{j1} unfolded distributions were used to put constrains on EFT Wilson coefficients from CP-even and CP-odd operators [19].

3.2 Measurements at 13.6 TeV

The ATLAS Collaboration published the fist measurement of the Higgs boson production cross section at 13.6 TeV performed in the $H \to ZZ^* \to 4l$ and $H \to \gamma\gamma$ decay channels and the combination [20]. The collected luminosity during the 2022 data taking phase is of 31.4 fb^{-1} for the $H \to \gamma\gamma$ analysis and 29.0 fb^{-1} for the $H \to ZZ^* \to 4l$ one. The observed (expected) fiducial cross section per channels are $\sigma^{\gamma\gamma}_{fid} = 76^{+14}_{-13}$ fb (67.6 $\pm$ 3.7 fb) and $\sigma^{4l}_{fid} = 2.8 \pm 0.74$ fb (3.67 $\pm$ 0.19 fb). The combined total cross section is 58.2 $\pm$ 8.7 pb, compatible with the SM expectation of 59.9 $\pm$ 2.6 pb [20].

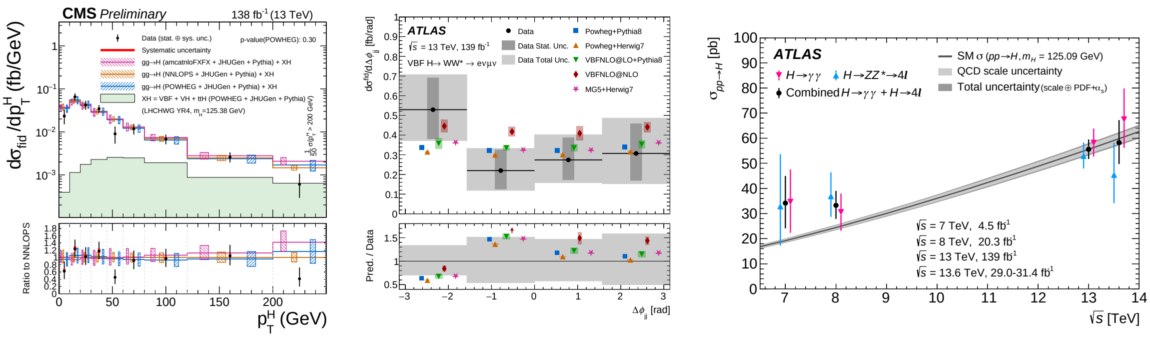

Figure 2: (left) Differential fiducial cross section measurements and comparison to the theoretical estimates for the p_T^H in the $H \to ZZ^* \to 4l$ decay channel performed by CMS [15]. (center) Differential fiducial cross section measurements and comparison to the theoretical estimates for the $\Delta\phi_{jj}$ in the $H \to WW^* \to 2l2\nu$ decay channel performed by ATLAS targeting the VBF production [19]. (right) Higgs boson production cross measurements in the $H \to ZZ^* \to 4l$ and $H \to \gamma\gamma$ and their combination as a function of the pp centre-of-mass energy performed by ATLAS [20].

4. Higgs boson Couplings

4.1 Production cross section and decay branching ratio: κ-framework interpretation

The production cross section measurements represent a good way to probe the strength of the Higgs boson coupling with the other Standard Model particles and test possible beyond SM effects. After 10 years from the discovery both ATLAS [21] and CMS [22] provided combined measurements of the Higgs boson couplings. The results provided by ATLAS in terms of cross section times branching ratio with respect to the Standard Model expectation showed an overall compatibility of 72%, while the CMS results were provided as signal strength for each production mode, with a compatibility of 3.1% and for each decay channel, with a compatibility of 30.1%. On top of those results, ATLAS updated the VH measurement $H \to WW^*$ decay channel, measuring $\sigma_{WH} \times B_{H\to WW^*} = 0.13^{+0.08}_{-0.07}$(stat.)$^{+0.05}_{-0.04}$(syst.) pb and $\sigma_{ZH} \times B_{H\to WW^*} = 0.31^{+0.09}_{-0.08}$(stat.)$\pm$0.03(syst.) pb [23]. CMS also updated their VBF measurement in $H \to b\bar{b}$ measuring a signal strength of $\mu_{VBF} = 0.97^{+0.53}_{-0.45}$ (2.4σ) [24].

Those results have been interpreted in terms of Higgs boson coupling strength modifiers κ in multiple scenarios. An interpretation assuming a universal coupling of vector bosons and fermions κ_V and κ_F has been performed, and also considering the coupling strength to W, Z, t, b, τ, μ and for

ATLAS also to the charm quark, independently. In particular, ATLAS tested two scenarios where κ_c was in one case fixed equal to κ_t and in the other case was floated, setting an upper limit on $kappa_c < 5.7$ at 95% CL [21]. While CMS published a separate result to measure the coupling with charm quark putting limits of $\kappa_c = [1.1, 5.5]$ at 95% CL [25].

4.2 Simplified Template Cross Section

A way to perform this measurement is in the *Simplified Template Cross Section* framework (STXS) [26], defining exclusive regions of the Higgs phase space (called STXS bins) based on its kinematics and of the particle and jets produced in association to identify the different production modes: p_T^H, N_{jets}, m_{jj}, p_T^V. The definitions of the STXS bins are motivated by maximising the experimental sensitivity and minimising the dependency on theoretical uncertainties. Different STXS Stages can be defined, corresponding to increasingly fine granularity, but not all the analyses are sensitive to all the STXS bins. The STXS measurement is performed defining a reco-level categorisation, which is chosen as close as possible to the STXS one to minimise the extrapolation dependency. ATLAS provided a joint measurement of 36 regions combining the results in the 5 observed decay channels, which show a good agreement with Standard Model with a p-value of 94% [21]. CMS recently studied the VH production in the $H \to b\bar{b}$ decay channels with the full Run 2 dataset, performing 8 STXS measurements [27].

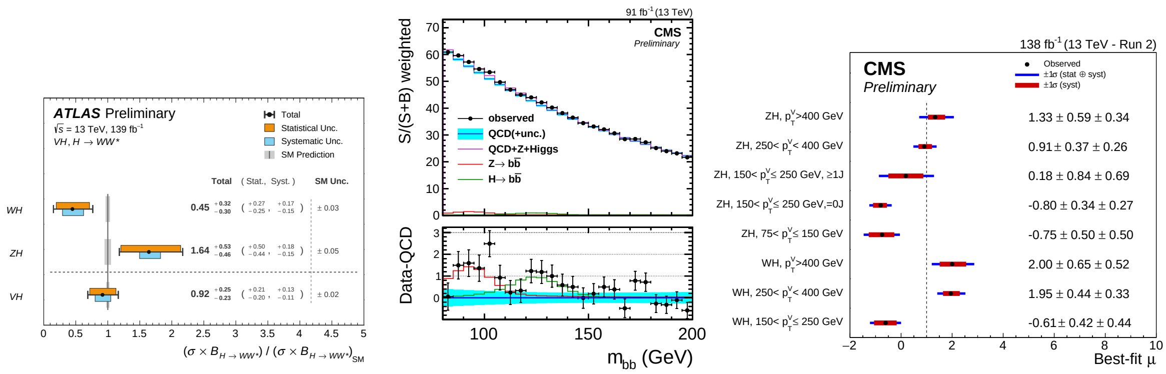

Figure 3: (left) Cross section times branching ratio with respect to the Standard Model expectation in the VH production in $H \to WW^*$ decay channel performed by ATLAS [23]. (center) Invariant mass distribution of bottom pairs measured by CMS for the VBF production in the $H \to b\bar{b}$ decay channel [24]. (right) Recent results in the VH production in $H \to b\bar{b}$ decay performed by CMS in 8 STXS bins [27].

4.3 Higgs boson rare and invisible decays

Finally several searches in unobserved Higgs decay channels have been performed with Run 2. In particular both ATLAS and CMS investigated the very rare decay of the Higgs boson into $Z\gamma$ final states. This is important to probe the Higgs boson properties and to validate SM over BSM theories. It was not observed yet, but with full Run 2 statistics both the experiments observed an excess of $\mu_{sig} = 2.0 \pm 1.0$ for ATLAS with a local significance of 2.2σ [28] and of $\mu_{sig} = 2.4 \pm 0.9$ for CMS with a local significance of 2.7σ [29]. Combing the information from ATLAS and CMS the first evidence of this process were claimed with a signal strength of $\mu_{sig} = 2.2 \pm 0.9$ with a local significance of 3.4σ and compatibility with Standard Model of 1.9σ [30].

The invisible Higgs decay is a way to probe a possible decay in WIMPs. It is characterised by the presence of missing transverse momentum E_T^{miss} in the interaction. The SM expectation of the branching ratio (BR) is $\mathcal{B}_{inv} = 0.1\%$ given by the $ZZ^* \rightarrow 4\nu$ process. Both ATLAS and CMS combining the seacrhes in different processes, set an upper limit on this BR of $\mathcal{B}_{inv} < 0.107$ at 95% CL [31] and $\mathcal{B}_{inv} < 0.15$ at 95% CL [32] respectively. They also interpreted those results to put constraints on WIMPs- or Dark Matter- nucleon scattering cross section as function of the candidate mass.

4.4 Higgs boson self-coupling

The Higgs boson self-coupling λ is a fundamental parameter of the Standard Model. For this reason ATLAS and CMS put lots of effort in trying to constraint the κ_λ parameter as much as possible studying the Di-Higgs processes and combining the results in the different final states ($b\bar{b}b\bar{b}$, $b\bar{b}\gamma\gamma$, $b\bar{b}\tau\tau$, $b\bar{b}ZZ^*$) all together. The best constraint reached by the ATLAS experiment comes from the combination of the double Higgs and single Higgs results: $-0.4 < \kappa_\lambda < 6.3$ at 95% CL [33]. From CMS Di-Higgs combinations the limits are $-1.24 < \kappa_\lambda < 6.49$ at 95% CL [22].

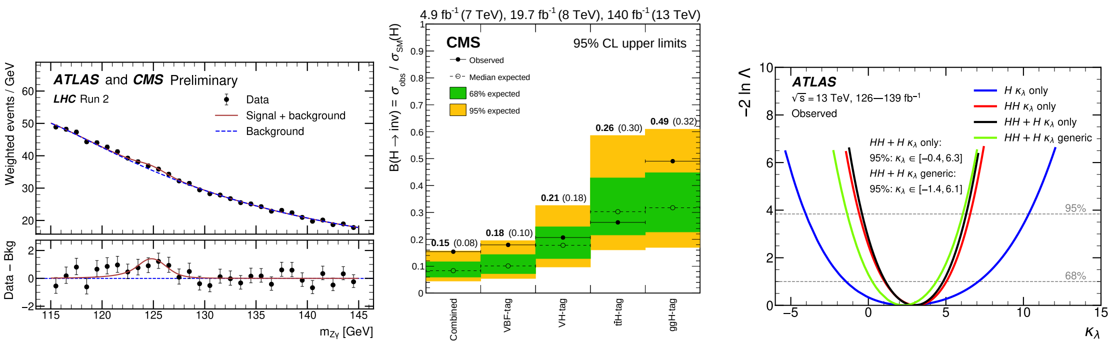

Figure 4: (left) The $Z\gamma$ invariant mass distribution of events from all ATLAS and CMS analysis categories [30]. (center) $H \rightarrow inv$ branching ratio measured by CMS in all the sensitive channels and their combination [32]. (right) Likelihood ratio distribution of κ_λ performed by ATLAS of the double Higgs and single Higgs searches and their combination [33].

5. Conclusion

The increase in integrated luminosity with Run2 lead to a lot of improvements in the precision of the Higgs boson property measurements and predicted Standard Model processes have been observed for the first time. All the measurements show a good agreement with the expectation and also several constraints on possible BSM couplings of the Higgs boson has been set with several analyses. Recently the first evidence of the off-shell production has been observed in the combination of the $H \rightarrow ZZ^* \rightarrow 4l + 2l2\nu$ decay channels by both ATLAS and CMS, as well as the combined effort between the two collaborations leaded to the first evidence of the Higgs boson decay in the $Z\gamma$ final state. Finally, the ATLAS experiment performed the first measurement of the Higgs boson production cross section at 13.6 TeV in the $H \rightarrow ZZ^* \rightarrow 4l$ and $H \rightarrow \gamma\gamma$ decay channels, opening a new era of measurements of the Higgs boson properties.

References

[1] ATLAS Collaboration, JINST **3** (2008), S08003

[2] CMS Collaboration, JINST **3** (2008), S08004

[3] ATLAS and CMS Collaboration, JHEP **08** (2016), 045 (*Preprint* [arXiv:1606.02266 [hep-ex]]).

[4] S. Heinemeyer *et al.* [LHC Higgs Cross Section Working Group], *Preprint* [arXiv:1307.1347 [hep-ph]].

[5] CMS Collaboration, Phys. Lett. B **805** (2020), 135425

[6] ATLAS Collaboration, Phys. Lett. B **843** (2023), 137880

[7] ATLAS Collaboration, Phys. Rev. Lett. **131** (2023) no.6, 061802

[8] ATLAS Collaboration, [arXiv:2304.09612 [hep-ex]].

[9] CMS Collaboration, Phys. Rev. D **108** (2023) no.3, 032013

[10] ATLAS Collaboration, [arXiv:2303.05974 [hep-ex]].

[11] CMS Collaboration, JHEP **07** (2023), 092

[12] ATLAS Collaboration, Eur. Phys. J. C **83** (2023) no.7, 563

[13] ATLAS Collaboration, Phys. Lett. B **846** (2023), 138223

[14] CMS Collaboration, Nature Phys. **18** (2022) no.11, 1329-1334

[15] CMS Collaboration, CMS-PAS-HIG-21-009 (https://cds.cern.ch/record/2839931)

[16] CMS Collaboration, JHEP **07** (2023), 091

[17] ATLAS Collaboration, JHEP **05** (2023), 028 doi:10.1007/JHEP05(2023)028

[18] ATLAS Collaboration, Eur. Phys. J. C **83** (2023) no.9, 774

[19] ATLAS Collaboration, Phys. Rev. D **108** (2023) no.7, 072003

[20] ATLAS Collaboration, ATLAS-CONF-2023-024 (https://cds.cern.ch/record/2859349/).

[21] ATLAS Collaboration, Nature **607** (2022) no.7917, 52-59 [erratum: Nature **612** (2022) no.7941, E24]

[22] CMS Collaboration, Nature **607** (2022) no.7917, 60-68

[23] ATLAS Collaboration, ATLAS-CONF-2022-067 (https://cds.cern.ch/record/2842519/).

[24] CMS Collaboration, CMS-PAS-HIG-22-009 (https://cds.cern.ch/record/2839932).

[25] CMS Collaboration, Phys. Rev. Lett. **131** (2023) no.6, 061801

PoS(LHCP2023)227

[26] N. Berger, C. Bertella, T. P. Calvet, M. Calvetti, V. Dao, M. Delmastro, M. Duehrssen-Debling, P. Francavilla, Y. Haddad and O. Kivernyk, *et al.* [arXiv:1906.02754 [hep-ph]].

[27] CMS Collaboration, CMS-PAS-HIG-20-001 (https://cds.cern.ch/record/2827421).

[28] ATLAS Collaboration, Phys. Lett. B **809** (2020), 135754

[29] CMS Collaboration, JHEP **05** (2023), 233

[30] CMS and ATLAS Collaboration, [arXiv:2309.03501 [hep-ex]].

[31] ATLAS Collaboration, Phys. Lett. B **842** (2023), 137963

[32] CMS Collaboration, Eur. Phys. J. C **83** (2023) no.10, 933

[33] ATLAS Collaboration, Phys. Lett. B **843** (2023), 137745